Philippine Journal of Science
152 (2): 591-604, April 2023
ISSN 0031 - 7683
Date Received: 29 Sep 2022

Nickel Electrodeposition Using Deep Eutectic Solvent-based Electrolyte

Eden May B. dela Peña*

Department of Mining, Metallurgical, and Materials Engineering,
University of the Philippines, Diliman Quezon City, NCR 1101 Philippines

While nickel (Ni) electroplating has been successfully performed using ionic liquids in the past, few studies have reported on the trench-filling characteristics of this process useful for electroforming Ni. This study aimed to deposit and characterize the electrodeposited nickel using an ethaline-based nickel-plating bath with and without ethylenediamine (en). The conductivity of the plating bath was improved, while viscosity was slightly reduced upon the addition of en. Cyclic and linear sweep voltammetry revealed that en acted as a suppressor, significantly reducing the bath's plating rate. The Hull cell was used to determine the optimum operating current density for each bath. The additive-bearing bath produced more compact deposits, better deposit grain morphology, and improved trench-filling (> 95% filling) characteristics compared to its additive-free counterpart. The enhanced super-filling characteristics may be explained by the differential acceleration curvature-enhanced accumulation acceleration (CEAC) model. SEM analysis showed that the deposits possessed a particulate or nodular structure, whereas EDS confirmed the presence of Ni in the deposit. The Ni deposited using the bath without additives had larger particulate grains than those using the additive-bearing bath. Higher Ni amounts were obtained in the additive-laden bath. The use of additives is a promising approach for improving the super-filling characteristics of ionic liquid plating baths.

Keywords: choline chloride, deep eutectic solvent, ionic liquid plating, nickel, plating additives

INTRODUCTION

Electroforming is an offshoot of the metal deposition process called electrodeposition or electroplating. In electroforming, a shape is formed by electrodepositing the metal on an electrically conductive model, referred to as the mandrel (Parkison 1998; McGeough 2014). Once the desired thickness is achieved, the electroformed metal is harvested *via* separation from the mandrel. Electroforming is considered an additive manufacturing technique, as the process involves the deposition of materials atom by atom. The thicknesses of electroformed products can range from 10 μm for foils to 50 mm for mold backings. The most popular electroformed metals are copper, nickel, silver, and gold (Parkison 1998).

*Corresponding author: ebdelapena@up.edu.ph

Electroforming is most applicable when extreme tolerances are necessary. Indeed, electroforming is considered one of the best technologies for precision metal fabrication, and its ability to replicate a surface with high fidelity is unmatched by most manufacturing processes. It is also useful for creating products that are lightweight and with complex shapes. Electroformed metals can be made with high purity while possessing good mechanical properties due to a fine-grained microstructure. Multiple layers of electroformed metals can also be created to produce structures with complex geometries such as grown-on flanges.

Though other more complex shapes are feasible from electroforming – including rocket thrust chambers, precision bellows, and MEMS – one major application

of the process is for creating 2D shapes such as screens, meshes, and filters (Parkison 1998). These can be used in a wide range of applications, such as industrial (*e.g.* textile printing screens, continuous centrifuge screens, filters), household (*e.g.* razors' screen), and energy (*e.g.* battery electrodes). The thickness of the mesh can be smaller than 10 µm, whereas apertures can be as small as 25 µm.

To create a mesh, a flat sheet mandrel is initially coated with a photoresist (Khan *et al.* 2017). Next, the pattern for the apertures is created *via* exposure either to UV or laser. The resist is stripped, subsequently creating trenches that outline the mesh, whereas the resist remains on the areas that will be apertures. Electrodeposition is then performed until the trench is filled. The trench can even be overfilled to create more unique shapes. The remaining resist is then stripped, and the electroformed mesh is separated from the mandrel. An important property for the creation of defect-free meshes would be the ability to deposit in narrow and high aspect-ratio trenches. Such will require good throwing power and effective trench-filling (also known as "super-filling") characteristics of the bath. Additionally, trench-filling electroplating processes are also important in the semiconductor industry for the fabrication of copper interconnects (West 2000). The success of these super-filling copper plating techniques depends largely on the use of organic additives (Andricacos *et al.* 1998).

To make defect-free electroformed screens, it is necessary that bottom-up filling occurs (Marro *et al*. 2017). This means that the deposition begins at the bottom of the trench and continues toward the top. Rapid deposition at the trench sides or at the top can cause voids to form. In aqueous solutions, the bottom-up filling was addressed through the clever use of additives. Additives are chemicals that are added to the plating bath to create a necessary property in the deposits. Some of the useful additives include brighteners and levelers.

Traditional electroforming uses an aqueous electrolyte. The major issue with aqueous electrolyte is that it has a narrow potential window, the possibility of hydrogen evolution and hydrogen embrittlement of deposit and substrate, and the need for complexing metal salts in solution using toxic agents such as cyanide (Abbot *et al*. 2017). A recent process approach to address such issues is ionic liquid electroplating. Ionic liquid electroplating uses ionic liquids (ILs) instead of the traditional aqueous or water-based electrolytes. ILs are molten at ambient temperatures and consist entirely of ionic counterparts (anion and cation) (Abbott and McKenzie 2006; Abbott *et al*. 2013). Past research proved that ILs offer major benefits when used as a plating bath compared to traditional aqueous electrolytes in electroplating. These benefits include: [i] high conductivity, [ii] wide potential windows, [iii] ability to deposit with very negative redox potential, [iv] high solubility of metal salts, [v] avoidance of water and metal/water chemistry, [vi] ability to deposit on passivating substrates, [vii] avoidance of complexants (*e.g.* cyanide), [viii] deposition of novel deposit architectures, and [ix] different possible formulations of the solution (Abbott *et al.* 2013). This new field of using ILs for metal deposition and surface modification is called ionometallurgical electroplating.

Researchers have only recently investigated the use of IL for electroplating. A considerable number of metals have already been deposited, from the traditional plated metals, such as Cu, Ni, Cr, Au, and Ag, to difficult-to-electrodeposit metals such as Al, Ti, W, Ta, and Mg (Andricacos 1998; West 2000; Abbott *et al*. 2013).

A popular misconception about the use of ILs in electroplating is the high process cost. This is reasonable as IL salts are more expensive than aqueous solutions. However, most of the cost of traditional electroplating is found in the cost of the metal salt used, and ILs can allow cheaper metal salt alternatives. Additionally, it has been reported that ionic liquid baths can last more than a year without degradation; hence, long-term top-up chemical and maintenance cost is much lower. Both these factors enhance the appeal of using ILs in electroplating (Abbott and McKenzie 2006; Abbott *et al.* 2017).

The recent introduction of water-stable deep eutectic solvents (DESs) has further lowered the barrier to ionic liquid plating (Abbott *et al*. 2013). DESs offer some advantages over traditional ILs – including simpler preparation (thus easier to mass produce in large batches), better availability, and less expensive. A popular DES is choline chloride (ChCl), a type of quaternary ammonium salt, mixed with a hydrogen bond donor such as urea or ethylene glycol. This mixture has been successfully used in plating different metals – i including pure metals such as Zn, Cr, Co, Cu, Sn, and Ni (Abbot *et al*. 2007a, 2008, Al-Murshedi *et al*. 2020; Alesary *et al.* 2019a, 2021), and alloys such as ZnSn (Abbot *et al*. 2007b; Alesary 2020), ZnNi (Lei *et al*. 2020) and CoZn (Mohammed *et al.* 2022). ChCl is also biodegradable making it an environment-friendly or "green" alternative to traditional plating that uses hazardous chemicals such as acids, bases, and cyanide (Haerens *et al*. 2009).

There are very few reports on electroforming using ionic liquid baths. In 2012, Ruan and Schuh reported on some preliminary work on electroforming Al-Mn alloys. They noted the benefits of using a pulsed current to improve the strength and ductility of the alloy. Clearly, more work is necessary to advance the field of ionic liquid electroforming.

There are several studies that have looked at nickel (Ni) electroplating using traditional ILs such

as 1-butyl-3-methylimidazolium dibutylphosphate (BMIM), and 1-butyl-1-methylpyrrolidinium bis(trifluoromethylsulfonyl)amide (BMPTFSA), as well as the more recent DES such as ethaline (ChCl:2EG), a mixture of ChCl and ethylene glycol at 1:2 molar ratio (Abbott *et al.* 2008; Zhu *et al.* 2009; Florea *et al.* 2010; Cherigui *et al.* 2017; Sebastian *et al.* 2018; Sun *et al.* 2019; Zheng *et al.* 2020). Some studies have also investigated the influence of additives on the properties of electroplated Ni from DESs. Abbot *et al*. (2008) reported that adding ethylenediamine (en) or acetyl acetonate (acac) to ethaline improved the structure of Ni deposits, whereas Juma *et al*. (2021) created mirror-finish Ni deposits by adding hydantoin to ethaline. Alesary *et al*. (2019b) noted that sodium bromide additions created bright and smooth Ni deposits in an ethaline bath.

However, no work has considered electroforming using ionic liquid baths to create mesh structures. As described above, the process of mesh electroforming requires filling deep structures such as trenches. But what could make ionic liquid electroplating particularly challenging in trenches is the nature of this material. ILs are generally viscous compared to other liquids of similar nature such as molecular liquids or high-temperature molten salts. Hence, diffusion is an important parameter for electrochemical processes in these solvents. Recent studies in mass transport in ILs have shown that diffusion does not obey Stoke's Law, and diffusion rates are significantly influenced by temperature (Taylor *et al.* 2011; D'Agostino *et al.* 2011). This suggests that mass transport in ILs occurs *via* a hole-jumping method rather than *via* classical diffusion motion (D'Agostino *et al.* 2011). The switch in mechanism for charge transport from hole mobility to ion mobility allows one to distinguish between an ionic or a molecular liquid. Furthermore, understanding the factors that affect hole mobility in ionic liquid may help in the design of more efficient liquid systems in the future.

Electrodeposition is also affected by the processes occurring within the electrical double layer and the adjacent diffusion layer. However, the relatively high viscosity of ILs impairs the necessary metal-ligand-anion interactions. Unfortunately, even the local solubility in the diffusion layer region is poorly understood, and metal deposition causes a high concentration of ligands close to the electrode substrate surface.

This research aims to investigate the trench-filling characteristics of an additive-free and an additive-laden nickel-based ionic liquid bath. To the best of the author's knowledge, this is likely one of the few reports reporting on this aspect of Ni ionic liquid plating. The plating bath will be based on ethaline, a DES consisting of a mixture of choline chloride and ethylene glycol. The additive tested is ethylenediamine (en), a proven additive for Ni plating (Abbot *et al*. 2008). Abbot *et al.* (2008) reported that adding en in the ethaline Ni bath resulted in greater leveling and decreased roughness; it also created a dull gray deposit. The different baths will be characterized, the plating process parameters will be determined using Hull cell experiments, and the morphology of the deposited metal will be characterized to determine important characteristics of the baths.

MATERIALS AND METHODS

Deep Eutectic Solvent Preparation

Ethaline (ChCl:2EG) was prepared using a 1:2 molar ratio mixture of choline chloride [$HOC_2H_4N(CH_3)_3Cl$] (ChCl) (Aldrich 99%) and ethylene glycol (EG) (Aldrich 99%). ChCl-based DES offers the widest potential window and stability, making it an ideal base for the plating bath (Maniam and Paul 2020). To make the bath, 0.2-mole nickel chloride dihydrate ($NiCl_2{\cdot}2H_2O$) was added to 1 L of ethaline. The additive used was ethylenediamine (en) (Sigma Aldrich), a known plate brightener. Initial tests on the additive-bearing solution showed that at en additions of less than 2.0 M, no appreciable change in the plating bath's electrochemical quality was observed. Some studies (Abbott *et al.* 2008; Zhu *et al.* 2009) have considered higher en concentrations, although the ideal operating condition would be to use additives at the minimum concentration where the desired effect is obtained. Hence, the additive concentration was set at 2.0 M. All chemicals were used as received. The mixtures were stirred in the stated proportions at 75 °C until a homogeneous, green solution formed for the additive-free DES, whereas a dark violet solution was observed in the additive-bearing DES, as shown in Appendix Figure A1.

Copper Trenches Preparation

The 1-cm^2 copper substrates were masked and patterned using photolithography. Afterward, the substrates were etched using $FeCl_3$, deionized water, and hydrochloric acid (HCl). The surface of copper substrates was further characterized using a 3D image in preparation for nickel deposition. Appendix Figure A2 shows the 3D image of the trenches, with line widths of 76 um (W) and 1 cm (L).

Electrochemical Analysis and DES Characterization

Viscosity measurement was conducted at varying temperatures using a rotational viscometer (VISCOTM-6800, Atago Co., Japan), employing an A1L setting (composed of A1 spindle type and L-type beaker) at 150 rpm. Electrical conductivity values at different temperatures were determined using a conductivity meter

(LAQUAact-EC120, Horiba, Japan) with a titanium-platinum black electrode (K = 1 cm^{-1} LAQUA 9382-10D, Horiba, Japan) as a probe. Both conductivity and viscosity measurements were conducted at a test temperature range of 25–40 °C.

Cyclic voltammetry (CV) and linear scan voltammetry (LSV) were done prior to electrodeposition experiments to assess the electrolyte's electrochemical behavior using a three-electrode system and potentiostat, as shown in Appendix Figure A3. LSV was conducted at more precise scan ranges to analyze specific electrochemical reactions.

A three-electrode apparatus was used consisting of glassy carbon (1-cm^2 surface area) as the working electrode, platinum (Pt, 2.5-cm^2 surface area) as the counter electrode, and silver (Ag) as the pseudo-reference electrode. The working electrode was prepared by washing it with deionized water (DI water). A solid pseudo-RE (*i.e.* Ag) is suitable since the difference in viscosity between DES and the electrolyte in a traditional reference electrode (*e.g.* Ag/AgCl/sat KCl) can affect ion mobility (Ismail *et al.* 2019, 2022). CV was performed at the potential range of –2.5 to 1.0 V_{Ag} (0 to –2.5 V_{Ag}; –2.5 to 1.0 $V_{Ag;}$ 1.0 to 0 V_{Ag}), a scan rate of 20 mV s^{-1}, and room temperature (25 °C) conditions using the Autolab Potentiostat (Model AUT 83997). LSV was performed at a range of 0 to –2.0 V_{Ag}, and a scan rate of 20 mV s^{-1}. Data analysis was subsequently performed using the Nova software.

Hull Cell Experiments

Hull cell experiments were conducted using a Yamamoto Hull cell. A 99.9% platinum anode (40.96 cm^2) was used, and a 99.8% copper sheet (30 cm^2) as the cathode. The cathode was polished using 800–2400 grit SiC and washed thoroughly with deionized water. A commercial power supply (Aim-TTi PL303QMD Quad-mode Dual) was used for the plating. The Hull cell experiments were conducted at 40 °C for a plating time of 4 h and at 0.5A applied current.

After the Hull cell electrodeposition, the substrates were rinsed with DI water and dried. The substrates were characterized using an optical microscope (Carl Zeiss, Primotech light microscope). The operating plating potential for each bath was then derived from the resulting plated metal on the Hull cell panel.

Nickel Electrodeposition Experiments and Characterization

The electrodeposition experiment was done using a power supply (Aim-TTi PL303QMD Quad-mode Dual power) and the three-electrode apparatus described above. The electrochemical cell has a minimum volume of 50 mL. The temperature of the cell was controlled and maintained at 40 °C using a hot plate. Nickel electrodeposition was performed at a constant potential. The electrodeposition time is fixed at 4 h.

At the end of the deposition time, the coated specimen was retrieved, rinsed in water, dried, and stored in a desiccator prior to analysis. A scanning electron microscope (SEM) was used to analyze the deposit's microstructure, whereas energy-dispersive X-ray (EDX) spectroscopy was used for compositional analysis.

RESULTS

Conductivity and Viscosity of DES

The conductivity and viscosity of the ethaline-Ni bath with (ChCl:2EG-Ni-en) and without (ChCl:2EG-Ni) additives are presented in Figure 1. It can be observed that the addition of ethylenediamine (en) caused an increase in both the electrolytes' conductivity and viscosity. There was a significant rise in the conductivity of the electrolyte after en addition at the tested temperatures (25–40 °C) – a more than 600% increase from about 58–60 to 370–398 mS/cm. As expected, the conductivity increased with increasing temperature, with the additive-bearing electrolyte exhibiting a slightly higher rate of increase than the additive-free electrolyte over the tested temperature range. The addition of en brought a slight increase in electrolyte viscosity at the tested temperature range (25–40 °C), about a 15% increase from 5–3.8 cP to 5.7–4.7 cP.

The higher conductivity found in the additive-bearing electrolyte indicates the easier passage of electricity through the electrolyte. On the other hand, a higher viscosity indicates difficulty in the diffusivity and mobility of ions. The conductivity of DES is governed by the mobility of ions, the primary charge carriers in this solution. Hence, conductivity is influenced by viscosity, *i.e.* the less viscous the solution, the more conductive it is. Hence, the significant increase (> 600%) in conductivity coupled with the slight increase (> 15%) in viscosity is certainly unexpected. The increase in viscosity should have resulted in a drop in solution conductivity due to the slower ion mobility. This suggests that the additive may have shifted the solution's conduction mechanism from ionic to electronic. Electronic conduction is significantly faster than ionic conduction. Due to the metallic halide content, the possibility of complex compound formation is possible. Such complexes may have been the conduit that allowed electron transfer, thereby causing the observed improvement in conductivity. This could also be due to a difference in Ni speciation in the bath after en addition. Abbott *et al.* (2008) confirmed that while $NiCl^{3-}$ is the main species present in the ethaline-Ni solution, the ligand

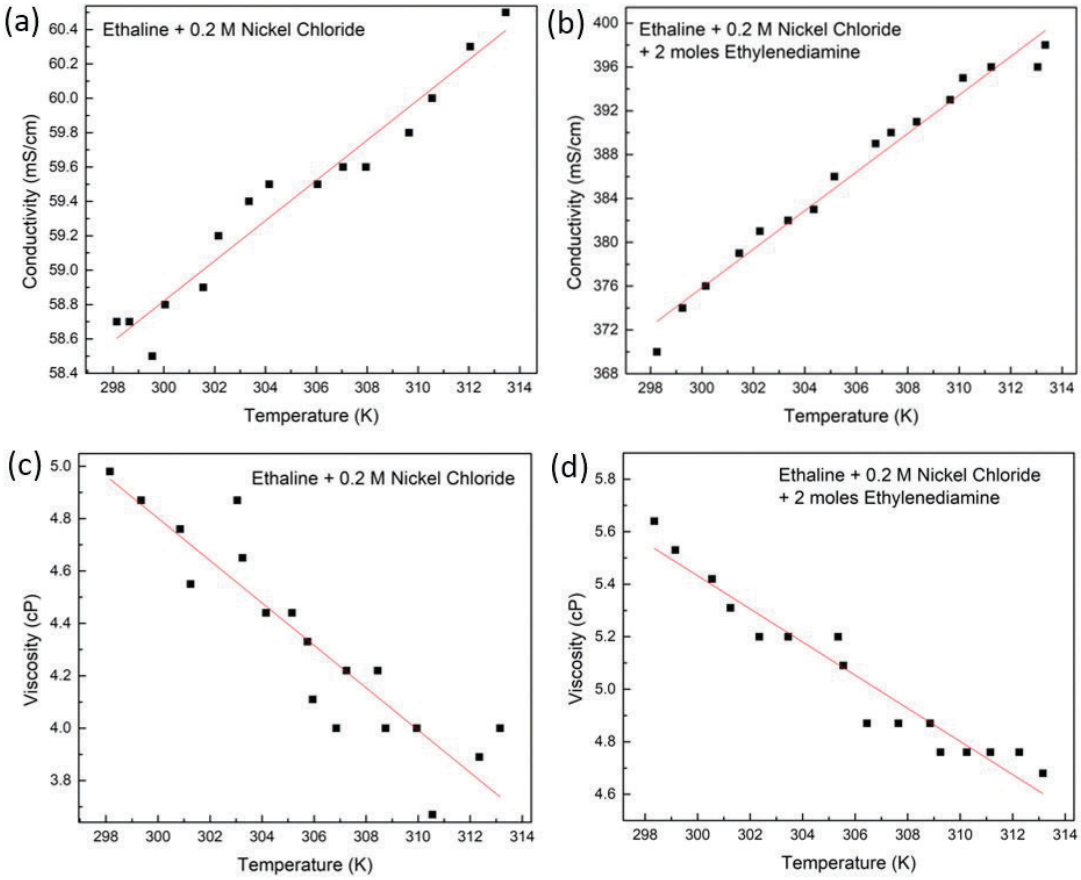

Figure 1. Conductivity of ChCl-based Ni plating bath without (a) and with (b) en additive. Viscosity of plating bath without (c) and with (d) en additive. Temperature range for both tests is from 25–40 °C (298–313 K).

complex, $[Ni(en)3]^{+2}$, may also be present, as indicated by the change in color of the bath (green to violet) after en addition.

Electrochemical Analysis

Figure 2 shows the cyclic voltammograms (CVs) for the ethaline-Ni bath with and without additives at room temperature (25 °C). The CVs reveal the effect of additives on the Ni plating bath.

The presence of peaks in the cathodic (negative) potential range suggests the reduction of Ni ions and the subsequent plating of Ni. Several research reported similar observations on the reduction of Ni ions in ILs (Bard *et al.* 2001; Tsuda *et al.* 2010; Huang and Zhang 2018). However, there is a significant difference in the cathodic behavior observed in the additive-free and additive-bearing plating baths. Firstly, the onset reduction potential in the ChCl:2EG-Ni-en (–1.3 V) was more negative compared to that in ChCl:2EG-Ni (–1.0 V), suggesting a higher energy barrier for Ni reduction in the additive-bearing bath. Secondly, the reduction current in ChCl:2EG-Ni-en was also considerably lower than in ChCl:EG-Ni, suggesting that the reduction kinetics was also reduced by en addition. The absence of the weak peak in the anodic scan indicates that the nickel plating did not oxidize and dissolve back in the ChCl:2EG-Ni bath. In contrast, the plated nickel in the ChCl:2EG-Ni-en bath appears to redissolve in the solution just above +0.75 V, as indicated by the rise in the anodic current. This indicates that there is a difference in the reversibility of the plating process in the two baths.

Linear sweep voltammetry (LSV) analysis was conducted, and the results are shown in Figure 3. In both solutions, the curve was generally smooth below 1.5 V. Consistent with the CV results, the LSV data show that the addition of en in 0.2M $NiCl_2 \cdot 2H_2O$ suppresses the reduction of Ni ions. The roughening of the plot beyond 1.5V may be due to side reactions such as water decomposition that produce hydrogen (Tsuda *et al.* 2010). Water was not added to the DES bath but may be unintentionally adsorbed from the environment since ethaline is naturally hygroscopic (Brusas and dela Pena 2021). While the influence of water on the Ni plating was not assessed in the current study,

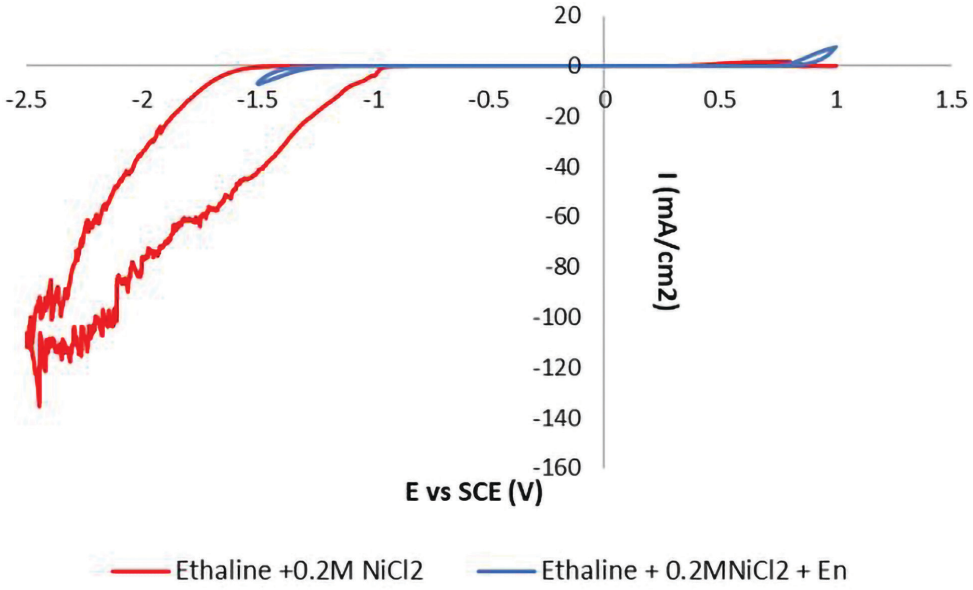

Figure 2. Cyclic voltammogram of ethaline with 0.2M $NiCl_2 \cdot 2H_2O$, and ethaline with 0.2M $NiCl_2 \cdot 2H_2O$ and en (scan rate: 20 mV s^{-1}; scan range: –2.5 to 1.0 V_{Ag}; temperature: 25 °C).

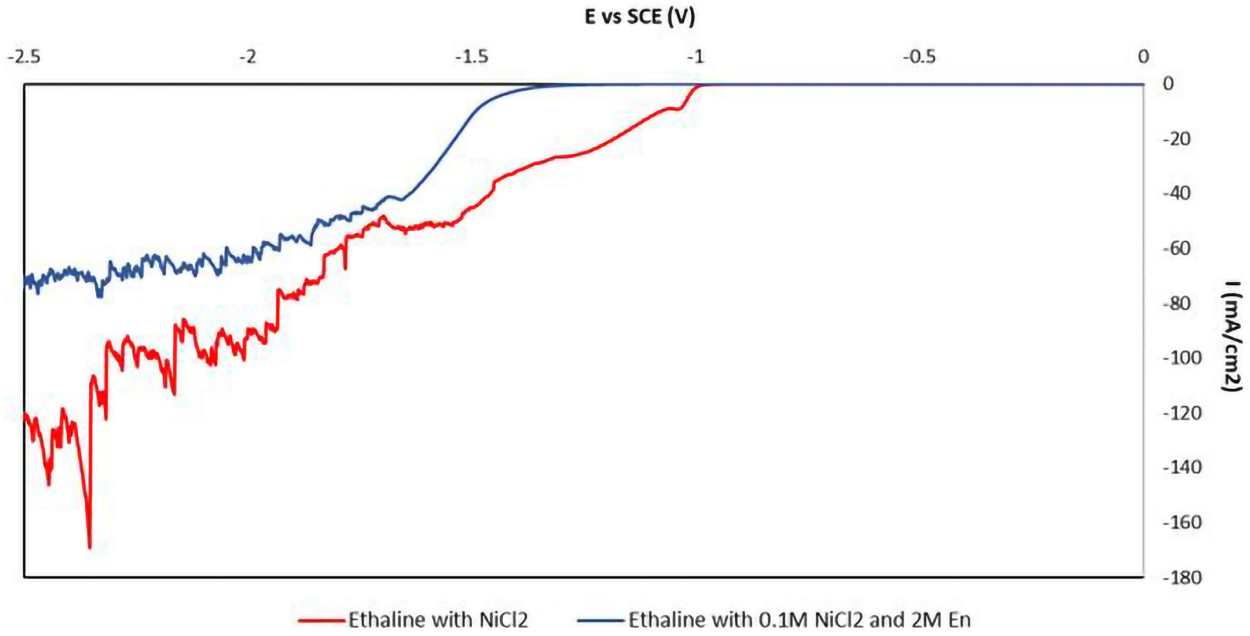

Figure 3. LSV voltammogram of ethaline and 0.2M $NiCl_2 \cdot 2H_2O$ and ethaline and 0.2M $NiCl_2 \cdot 2H_2O$ with en. (scan rate: 20 mV s^{-1}; scan range: 0 to –2.0 V_{Ag}; temperature: 25 °C).

previous works have indicated that this water uptake can reduce viscosity, enhance electrical conductivity, and decrease the electrochemical window of ethaline and will influence the speciation of the metal salt in the ionic liquid (Ismail 2020, 2022). Hence, it is expected that water addition will influence metal plating using DES-based plating baths (Ismail 2020, 2022).

The decrease in Ni's reduction rate correlates well with the increase in viscosity of the DES but contradicts the increase in conductivity brought about by en addition. This seems to imply that Ni's plating rate is strongly concentration-dependent and influenced by ion diffusion rather than charge-transfer mechanisms. Abbott *et al.* (2008) suggested that such observations may be related

to the differences in ligand activity between the two baths. En acts as a strong ligand for various transition metals, including Ni. En binds Ni ions and forms a stable Ni complex, thereby suppressing the metal's ability to nucleate and reducing the overall plating rate. A minimum amount of en (*i.e.* 2 moles/L) was needed to observe an appreciable influence on the bath's electrochemical properties. This suggests that a critical volume of additive is necessary to obtain the desired suppressing effect.

Hull Cell Experiments

Hull cell experiments were conducted to determine the practical plating current density. Shown in Figure 4 are the substrates after electrodeposition using the additive-free and additive-laden DES. The Ni deposit appears black, similar to reports by Abbot *et al.* (2008). The plated Ni using the additive-free plating bath appears thin, whereas those from the additive-bearing appear more uniform.

The Hull cell substrates were visually and microstructurally assessed to judge the quality of the electrodeposit. Based on the coverage of the nickel deposit, good plating coverage was obtained at 25.5 and 12.5 mA cm^{-2} for the ChCl:2EG-Ni and ChCl:2EG-Ni-en baths, respectively. The results again show that the operating plating current was reduced when the additive was added to the ionic liquid plating bath, consistent with the results of the electrochemical analysis.

Nickel Electrodeposition on Trenches and Microstructural Analysis

Using the identified plating currents from the Hull cell experiments, nickel was electrodeposited on copper using the two types of plating baths. Actual photographs of the plated samples are shown in Figure 5a and b. Again, the deposit appears black, consistent with previous studies (Abbott *et al.* 2008). Visually, the Ni deposited from ChCl:2EG-Ni looks porous and nonadherent, as well as exhibited poor coverage. In contrast, the specimen plated using ChCl:2EG-Ni-en possessed a uniformly coated surface (complete coverage), with the deposit appearing dense and compact. The average plating efficiency of the additive-free bath was 28.6%, and en addition slightly enhanced the efficiency to 35.2%. The plating thickness of ChCl:2EG-Ni was 35.9 ± 8.5 µm, whereas that of ChCl:2EG-Ni-en was 21.6 ± 3.2 µm.

Further comparisons of the Ni plating from the different baths can be made from the SEM images shown in Figures 5c–j. Figures 5c–f provide a view of the Ni-plated trenches. Figures 5c (low magnification) and e (high magnification) correspond to Ni deposited using the DES without additives, and Figures 5d and f are for the NI plated with en. Again, the black powdery deposit corresponds to Ni. The images of these Ni-filled trenches show a distinct difference in the trench-filling characteristics of the two baths. In the ChCl:2EG-Ni specimen, the trench was not entirely filled with the plated metal. The Ni deposit appeared chunky and discontinuous. In contrast, the ChCl:2EG-Ni-en specimen exhibited uniformly filled trenches. The Ni deposit is granular but generally finer and more compact compared to its additive-free counterpart. Evidently, the filling quality of the ChCl:2EG-Ni bath was significantly lower compared to ChCl:2EG-Ni-en. A quick estimate shows only about 70% super-filling and plating coverage in ChCl:2EG-Ni, compared to a remarkable > 98% in ChCl:2EG-Ni-en.

Figures 5g–j are higher magnification SEM images of the Ni deposit from the two baths. Figures 5g and i correspond

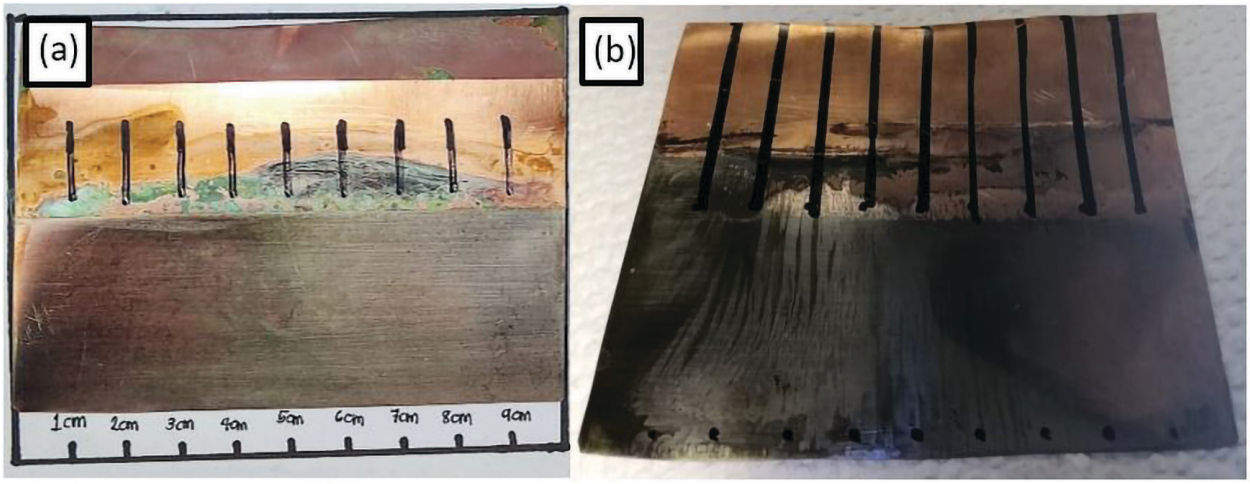

Figure 5. Actual specimen photographs of Ni electroplated (a) without and (b) with additives in the electrolyte. Corresponding SEM images of Ni electroplated without (c, e, g, and i) and with additives (d, f, h, and j): trench view (c and f) and planar/surface view (g–j). EDX spectra of the nickel deposit (k) without and (l) with additives

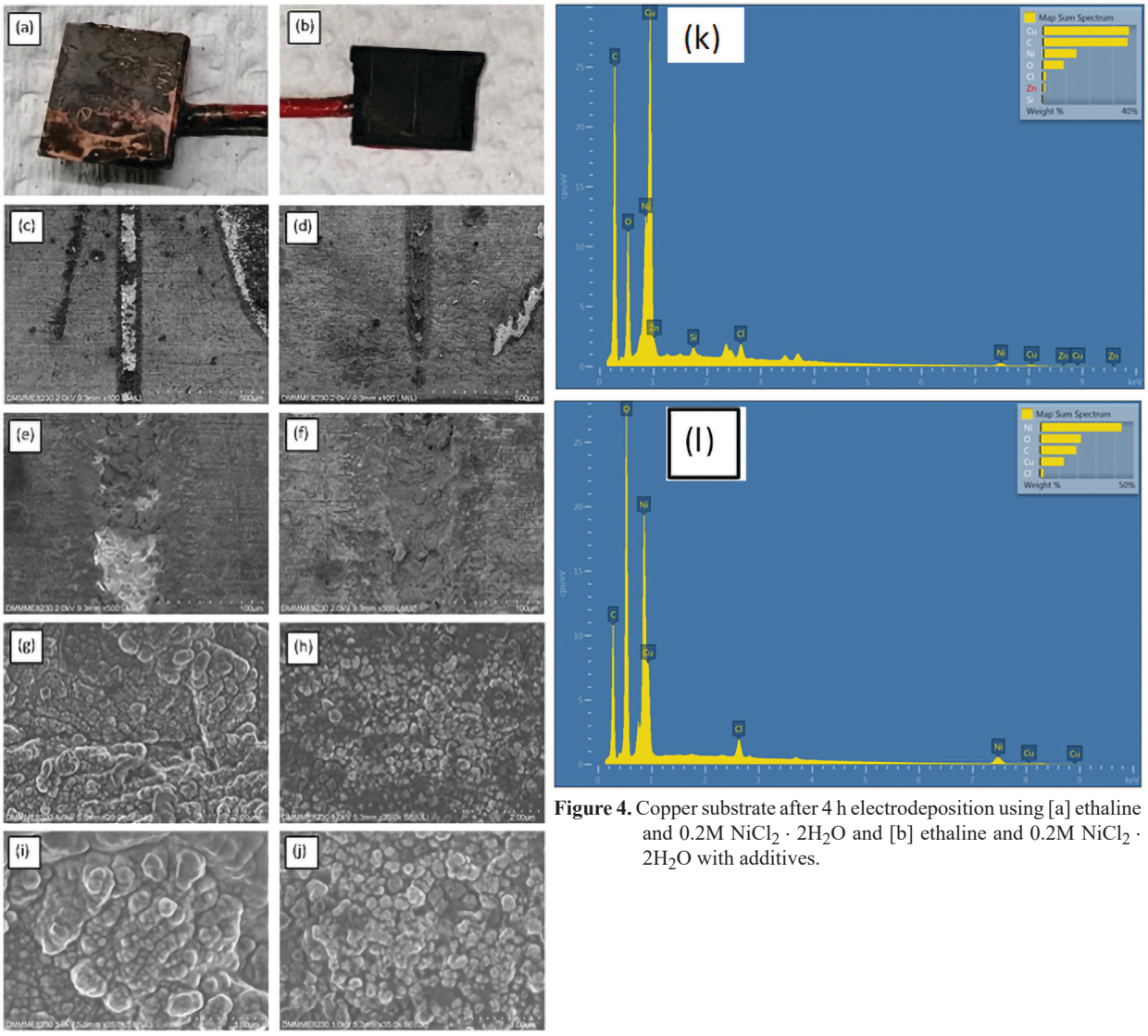

Figure 4. Copper substrate after 4 h electrodeposition using [a] ethaline and 0.2M $NiCl_2 \cdot 2H_2O$ and [b] ethaline and 0.2M $NiCl_2 \cdot 2H_2O$ with additives.

to the ChCl:2EG-Ni specimen, whereas Figures 5h and j are for the ChCl:2EG-Ni-en specimen. The Ni deposit from both baths possesses a particulate or nodular nature, again consistent with the literature (Abbott *et al.* 2008). The plated metal from ChCl:2EG-Ni appeared rough showing large particulate grains, whereas that from ChCl:2EG-Ni-en exhibited finer grains with a more uniform size distribution. Voids were also not prevalent in the deposit from ChCl:2EG-Ni-en, suggesting a compact or dense structure.

Figures 5k and j show the corresponding EDX spectrum of ChCl:2EG-Ni-en and ChCl:2EG-Ni-en specimens, respectively. The results confirm the presence of several elements at the plated surface. Copper and zinc were detected and likely originated from the brass substrate. Ni was also found in both specimens, confirming the success of electroplating. Oxygen, which could come from surface oxidation, and chlorine, which originated from the bath, were also present. The Ni signal was higher in the deposit using ChCl:2EG-Ni-en compared to that of ChCl:2EG-Ni, suggesting higher Ni amounts in the plating from ChCl:2EG-Ni-en and confirming the deposit's dense qualities.

DISCUSSION

En is a brightener, which stabilizes metal ions to form a stable complex (Abbott *et al.* 2008; Cherigui *et al.* 2017). The presence of this metal ion complex reduces the bath's plating rate by slowing down deposit nucleation, consistent with the results of the electrochemical tests on the bath. Though the addition of en reduced the bath's plating current, it also encouraged better

microstructural morphology *via* grain refinement of the deposit. Fine deposit grains often lend themselves to improved appearance and better substrate adhesion and mechanical properties. Indeed, the brightener's effect on the microstructure was confirmed by SEM images showing a finer, more compact grain morphology in the deposit from the additive-bearing bath compared to that of the additive-free bath.

The trench-filling or super-filling abilities of metals plated from ILs are rarely reported, and, as far as the author's knowledge, this is the first report on the super-filling abilities of an ionic-liquid-based Ni plating bath. This study shows that the additive-free ethaline-based Ni plating bath had poor trench-filling characteristics. Deposits were observed to be coarse and loose, likely contributing to their inability to adhere to the trench walls. The study further confirms that improvement of the bath's super-filling characteristics can be achieved through the use of appropriate additives such as en.

Though the mechanism for the improved trench-filling characteristics of the bath after en addition still needs to be ascertained, current mechanisms proposed for additive-enhanced super-filling behavior in aqueous baths may be considered. Two popular models may be considered: the differential inhibition model and the differential acceleration curvature-enhanced accumulation acceleration (CEAC) model.

The differential inhibition model is the first mechanism proposed to explain super-filling and is essentially based on the theory of leveler action (Andricacos 1999; Deligianni *et al*. 2000; West 2000). In this model, a strong leveler is believed to readily adsorb at the exposed surfaces found in the upper portions of the ridge. Consequently, the leveler inhibits metal deposition in these covered areas. On the other hand, trench bottoms remain free of the leveler since it takes time for the molecule to diffuse to and adsorb in these regions. Therefore, trench bottoms will have less inhibition, and plating is encouraged. One characteristic of leveler-dominated baths is creating plating deposits with high impurity content since levelers are incorporated in the deposit.

Moffat *et al.* (2000, 2002) proposed the more recent differential acceleration CEAC model. The CEAC explains the existence of an accelerator catalyst complex present in the suppressor-accelerator containing electrolytes (see Appendix Figure A4). This catalyst is adsorbed at specific regions on the substrate having a concave curvature, essentially found at trench bottoms, and promoting accelerated metal deposition. As the hole steadily fills up with the metal and less of the trench area is exposed, lesser amounts of the catalyst accumulate in the region. Deposition, which is limited by the steadily declining amount of catalyst in the trench, continues until the hole is completely filled. The CEAC model has a very good correlation with actual deposit profiles and is applicable even for other systems such as gold and silver plating (Baker *et al.* 2003).

The differential inhibition model may not be appropriate to describe en's leveling effect on the plating deposit. En is not supposed to be readily adsorbed at the substrate's surface but is expected to react with the Ni ion and exist as a complex in the bath. Hence, the CEAC appears to be the more appropriate model, considering that the model is based on the existence of an additive-based complex necessary to stimulate the super-filling action. The confirmation of this hypothesis requires further studies.

CONCLUSION

In this study, nickel was successfully plated using an ethaline-based Ni bath, and the trench-filling characteristics of the baths with and without ethylenediamine (en) were assessed. Some important conclusions from this work include:

i. Both additive-free and additive (en)-bearing DESs can be used to deposit nickel on the copper substrate.
ii. En addition improved the bath's conductivity while increasing viscosity. Electrochemical analysis revealed that en induced the suppression of Ni plating kinetics, likely due to the formation of stable metal complexes that inhibits deposit nucleation.
iii. Based on the quality of the plated Ni from the Hull cell experiments, the best operating plating current density for the two plating baths was identified: 25.5 mA/cm^2 for the additive-free bath and 17.5 mA/cm^2 for the en-bearing plating bath.
iv. Although the morphology of the deposits from the additive-free and additive-laden bath is generally similar, showing a nodular grain structure, the addition of en made the deposit finer, more even, and more compact. This confirmed that en is a strong suppressing agent and acts as a brightener in the DES bath.
v. En addition significantly enhanced the super-filling characteristics of the DES bath. The mechanism of the additive-induced super-filling is still to be determined, although likely explained by the differential acceleration CEAC model.

ACKNOWLEDGMENTS

This work was funded by the University of the Philippines (UP) System Enhanced Creative Work and Research Grant (ECWRG-2020-1-2-R). The author would also like to acknowledge the assistance of Ms. Salvacion Orgen and Mr. Patrick Arboleda from the SETLab (Sustainable Electrochemical Technologies Laboratory) of the College of Engineering, UP Diliman.

NOTES ON APPENDICES

The complete appendices section of the study is accessible at https://philjournsci.dost.gov.ph

REFERENCES

ABBOTT AP, MCKENZIE KJ. 2006. Application of ionic liquids to the electrodeposition of metals. Phys. Chem. 8: 4265–4279.

ABBOTT AP, MCKENZIE KJ, RYDER KS. 2007a. Electropolishing and Electroplating of Metals Using Ionic Liquids Based on Choline Chloride. ACS Sym. p. 186–197.

ABBOTT AP, CAPPER G, MCKENZIE KJ, RYDER KS. 2007b. Electrodeposition of zinc–tin alloys from deep eutectic solvents based on choline chloride. J Electroanal Chem 599: 288–294.

ABBOTT AP, TTALIB KEL, RYDER KS, SMITH EL. 2008. Electrodeposition of nickel using eutectic based ionic liquids. Transactions of IMF 86(4): 234–240.

ABBOTT A, FRISCH G, RYDER K. 2013. Electroplating Using Ionic Liquids. Annual Review of Materials Research 43: 335–358.

ABBOTT AP, ENDRES F, MACFARLANE DR. 2017. Why Use Ionic Liquids for Electrodeposition? In: Electrodeposition from Ionic Liquids. Endres F, Abbott A, MacFarlane D eds. Weinheim, Germany: Wiley-VCH

ALESARY HF, CIHANGIR S, BALLANTYNE AD, HARRIS RC, WESTON DP, ABBOTT AP, RYDER KS. 2019a. Influence of additives on the electrodeposition of zinc from a deep eutectic solvent. Electrochim Acta 304: 118–130.

ALESARY HF, KHUDAIR AF, RFAISH SY, ISMAIL HK. 2019b. Effect of Sodium Bromide on the Electrodeposition of Sn, Cu, Ag, and Ni from a Deep Eutectic Solvent-Based Ionic Liquid. J. Electroanal. Chem. 14: 7116–7132.

ALESARY HF, ISMAIL HK, SHILTAGH NM, ALATTAR RM, AHMED LM, WATKINS MJ, RYDER KS. 2020. Effects of additives on the electrodeposition of ZnSn alloys from choline chloride/ethylene glycol-based deep eutectic solvent. J Electroanal Chem 874: 114517.

ALESARY HF, ISMAIL HK, ODDA AH, WATKINS MJ, MAJHOOL AK, BALLANTYNE AD, RYDER KS. 2021. Influence of different concentrations of nicotinic acid on the electrochemical fabrication of copper film from an ionic liquid based on the complexation of choline chloride-ethylene glycol. J Electroanal Chem 897: 115581.

AL-MURSHEDI AYM, AL-YASARI A, ALESARY HF, ISMAIL HK. 2020. Electrochemical fabrication of cobalt films in a choline chloride–ethylene glycol deep eutectic solvent containing water. Chem Papers 74(2): 699–709.

ANDRICACOS PC, UZOH C, DUKOVIC JO, HORKANS J, DELIGIANNI H. 1998. Damascene Copper Electroplating for Chip Interconnections. IBM J Res & Dev 42: 567–574.

ANDRICACOS PC. 1999. Copper On-chip Interconnections: a Breakthrough in Electrodeposition to Make Better Chips. Electrochem Soc Interface 8(1): 32–37.

BAKER BC, FREEMAN M, MELNICK B, WHEELER D, JOSELL D, MOFFAT TP. 2003. Superconformal Electrodeposition of Silver from a KAG(CN)2-KCN-KSeCN Electrolyte. J Electrochem Soc 150(2): C61–C66.

BARD AJ, FAULKNER LR, BARD A, FAULKNER L. 2001. Electrochemical Methods: Fundamentals and Applications, 2nd Ed. New York: Wiley.

BRUSAS J, DELA PENA EM. 2021. Hygroscopicity of 1:2 Choline Chloride: Ethylene Glycol Deep Eutectic Solvent: A Hindrance to its Electroplating Industry Adoption. J Electrochem Sci Tech 12: 10.33961/jecst.2020.01522

CHERIGUI EAM, SENTOSUN K, BOUCKENOOGE P, VANROMPAY H, BALS S, TERRYN H, USTARROZ J. 2017. Comprehensive study of the electrodeposition of nickel nanostructures from deep eutectic solvents: self-limiting growth by electrolysis of residual water. J Phys Chem C 121: 9337–9347.

D'AGOSTINO RC, HARRIS AP, ABBOTT LF, GLADDEN MD. 2011. Molecular motion and ion diffusion in choline chloride based deep eutectic solvents studied by 1H pulsed field gradient NMR spectroscopy. Phys Chem Chem Phys 13(48): 21383–21391.

DELIGIANNI H, HORKANS, J, KWIETNIAK K, DUKOVIC JO, ANDRICACOS PC, BOETTCHER S, SEO S-C, LOCKE P, SIMON A, SEYMOUR S, MALHOTRA S. 2000. Model in Superfilling in Damascene Electroplating: Comparison of Experimental Feature Filling with Model Predictions, Electrochemical Processing. In: ULSI Fabrication III. PC Andricacos, PC Searson, C Redsema-Simpson, P Allongue, JL Stickney, GM Oleszek eds. PV 2000(8): 145–149.

FLOREA A, ANICAI L, COSTOVICI S, GOLGOVICIC F, VISAN T. 2010. Ni and Ni alloy coatings electrodeposited from choline chloride-based ionic liquids—electrochemical synthesis and characterization. Surf Interface Anal 42: 1271–1275.

HAERENS K, MATTHIJS E, CHMIELARZ A, VAN DER BRUGGEN B. 2009. The use of ionic liquids based on choline chloride for metal deposition: a green alternative? Journal of Environmental Management 90(11): 3245–3252.

HUANG P, ZHANG Y. 2018. Electrodeposition of Nickel Coating in Choline Chloride-Urea Deep Eutectic Solvent. Int J Electrochem Sci 13: 10798–10808.

ISMAIL HK. 2020. Electrodeposition of a mirror zinc coating from a choline chloride-ethylene glycol-based deep eutectic solvent modified with methyl nicotinate. J Electroanal Chem 876: 114737.

ISMAIL HK. 2022. A comparative study of the formation, and ion and solvent transport of polyaniline in protic liquid-based deep eutectic solvents and aqueous solutions using EQCM. Electrochim Acta 418: 140348.

ISMAIL HK, ALESARY HF, AL-MURSHEDI AYM, KAREEM JH. 2019. Ion and solvent transfer of polyaniline films electrodeposited from deep eutectic solvents *via* EQCM. J Solid State Electrochem 23(11): 3107–3121.

ISMAIL HK, QADER IB, ALESARY HF, KAREEM JH, BALLANTYNE AD. 2022. Effect of Graphene Oxide and Temperature on Electrochemical Polymerization of Pyrrole and Its Stability Performance in a Novel Eutectic Solvent (Choline Chloride–Phenol) for Supercapacitor Applications. ACS Omega 7(38): 34326–34340.

JUMA JA, ISMAIL HK, KARIM WO, SALIH SJ. 2021. High quality mirror finish fabrication of nickel electrodeposited using hydantoin from a mixture of choline chloride-ethylene glycol. Arab J Chem 14(3): 102966.

KHAN A, LEE S, T. JANG Z. XIONG, ZHANG C, TANG J, GUO LJ, LI WD. 2017. Scalable Solution-processed Fabrication Strategy for High-performance, Flexible, Transparent Electrodes with Embedded Metal Mesh. J Vis Exp. 23(124): 56019.

LEI C, ALESARY HF, KHAN F, ABBOTT AP, RYDER KS. 2020. Gamma-phase Zn-Ni alloy deposition by pulse-electroplating from a modified deep eutectic solution. Surf Coat Technol 403: 126434.

MANIAM KK, PAUL S. 2020. Progress in Electrodeposition of Zinc and Zinc Nickel Alloys Using Ionic Liquids. Appl Sci 10: 5321.

MARRO JB, OKORO CA, OBENG YS, RICHARDSON KC. 2017. The Impact of Organic Additives on Copper Trench Microstructure. J Electrochem Soc 164(9): D543–D550.

MCGEOUGH JA. 2014. Electroforming. In: The International Academy for Production Engineering, Laperrière L, Reinhart G eds. CIRP Encyclopedia of Production Engineering. Berlin-Heidelberg: Springer.

MOFFAT TP, BONEVICH JE, HUBER WH, STANISHEVSKY A, KELLY DR, STAFFORD GR, JOSELL D. 2000. Superconformal Electrodeposition of Copper in 500-90 nm Features. J Electrochem Soc 147(12): 4524–4535.

MOFFAT TP, WHEELER D, WITT C, JOSELL D. 2002. Superconformal Electrodepositon Using Derivatized Substrates. Electrochem and Solid-State Lett 5: C110–C112.

MOHAMMED ZJ, ALESARY HF, AHMED LM. 2022. A Study of the Effects of Water on the Electrochemical Properties and Characterization of Co-Zn Alloys from a Deep Eutectic Solvent. Egyptian J Chem 65(6): 255–267.

PARKISON R. 1998. Electroforming – a unique metal fabrication process. Nickel Development Institute Technical Series 10 084. Accessible at www.nickelinstitute.org

RUAN S, SCHUH C. 2012. Towards electroformed nanostructured aluminum alloys with high strength and ductility. Journal of Materials Research 27(12): 1638–1651.

SEBASTIAN P, GIANNOTTI MI, GÓMEZ E, FELIU JM. 2018. Surface sensitive nickel electrodeposition in deep eutectic solvent. ACS Appl Energy Mater 1: 1016–1028.

SUN C, ZENG J, LEI H, YANG W, ZHANG Q. 2019. Direct electrodeposition of phosphorus-doped nickel superstructures from choline chloride−ethylene glycol deep eutectic solvent for enhanced hydrogen evolution catalysis. ACS Sustain Chem Eng 7: 1529–1537.

TAYLOR AW, LICENCE P, ABBOTT AP. 2011. Non-classical diffusion in ionic liquids. Phys Chem Chem Phys 13: 10147–10154.

TSUDA T, BOYD LE, KUWABATA S, HUSSEY CL. 2010. Electrochemistry of Copper(I) Oxide in the 66.7–33.3 mol % Urea–Choline Chloride Room-temperature Eutectic Melt. J Electrochem Soc 157(8).

WEST AC. 2000. Theory of Filling of High-aspect Ratio Trenches and Vias in Presence of Additives. Journal of The Electrochemical Society 147(1): 227–232.

ZHENG Y, ZHOU X, LUO Y, YU P. 2020. Electrodeposition of nickel in air-and water-sTable 1-butyl-3-methylimidazolium dibutylphosphate ionic liquid. RSC Adv 10: 16576–16583.

ZHU YL, KOZUMA Y, KATAYAMA Y, MIURA T. 2009. Electrochemical behavior of Ni(II)/Ni in a hydrophobic amide-type room-temperature ionic liquid. Electrochim Acta 54: 7502–7506.

APPENDICES

Figure A1. Ethaline-nickel chloride electrolyte (left) and ethaline-nickel chloride-ethylenediamine plating bath (right).

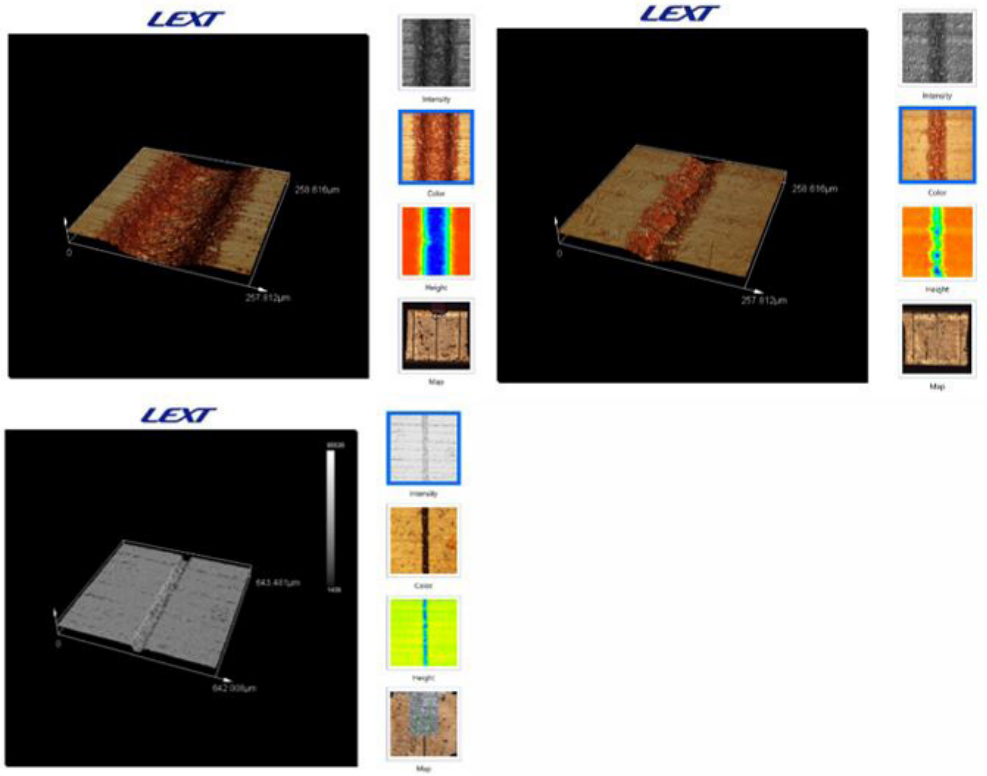

Figure A2. 3D image of copper trenches.

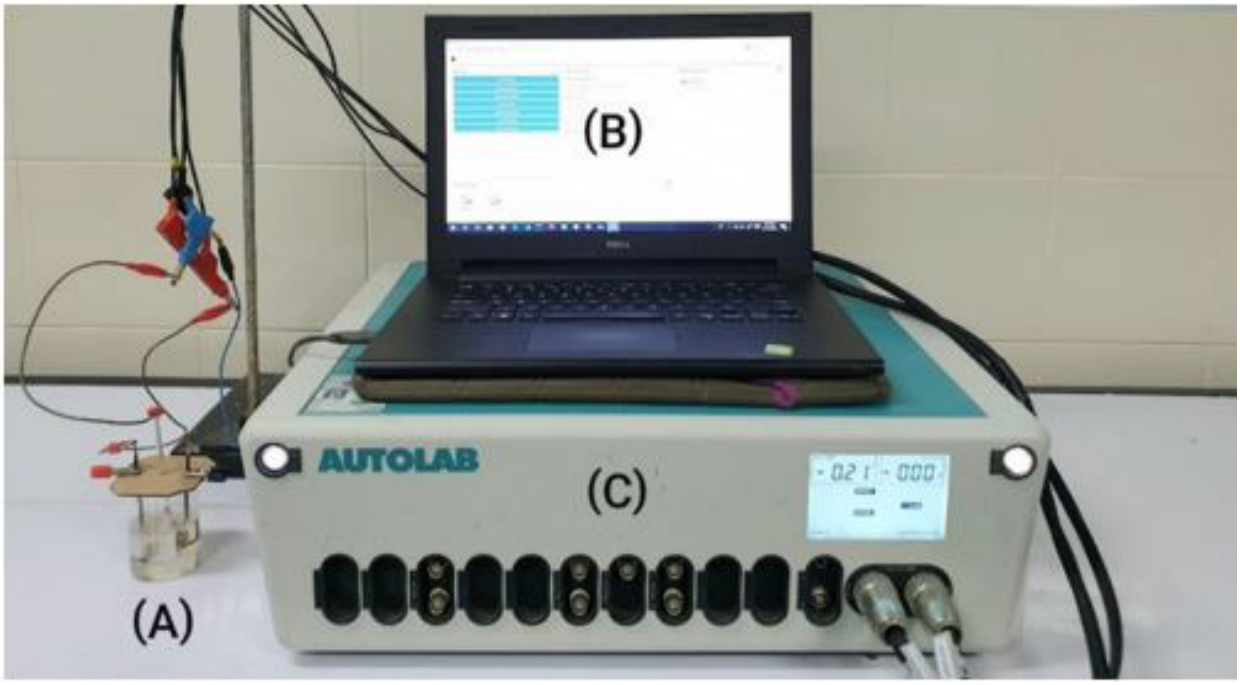

Figure A3. Three-electrode system (a), nova software (b), and electrochemical system/potentiostat (c) for polarization experiment.

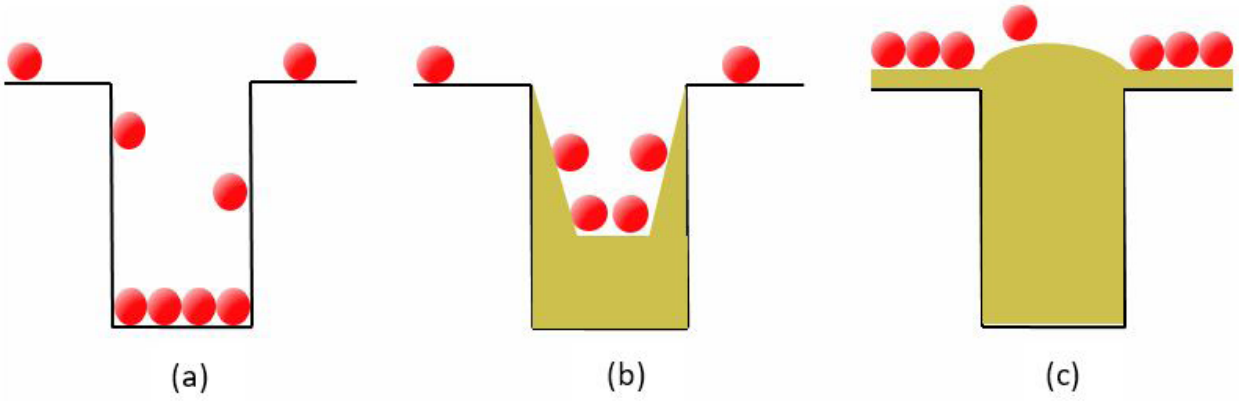

Figure A4. CEAC model explains that [a] additive complex (red circle) accumulates at the concave surfaces found at recesses. [b] The molecule complex accelerates metal deposition in these areas until the trench is filled. [c] At the top a change in surface curvature is experienced and complex diffuses to lower regions to promote leveling.